Summary: An inorganic hybrid material was produced using a polysiloxane binder and metal-oxo-clusters which were derived from sol-gel precursors. The continuous phase is composed of an elastomeric polysiloxane functionalized with cycloaliphatic epoxide groups. Pendant alkoxy silane groups serve as a coupling agent to form a network between the metal-oxo-clusters and the crosslinked polysiloxane. Methyl, cyclopentyl, and cyclohexyl substituted polysiloxanes were formulated with a variety of sol-gel precursors (tetraethylorthosilicate oligomers, titanium(IV) *iso*-propoxide, zirconium(IV) propoxide, and zinc acetate). Phase-modulated FT-IR, X-ray photoelectron spectroscopy, solid state ^{29}Si NMR, and solid state ^{13}C NMR were used to investigate the internal structure of the mixed metal-oxo/silicon-oxo colloids prepared within the cured polysiloxane matrix. Results indicate that the cycloaliphatic groups inhibit the complete hydrolysis and condensation of the pendant triethoxysilane group and reaction of the sol-gel precursors. Analysis also indicated that the metal-oxo-clusters were comprised of mixed species of sol-gel precursors resulting in hetero-bonded (Si–O–Metal) colloids.

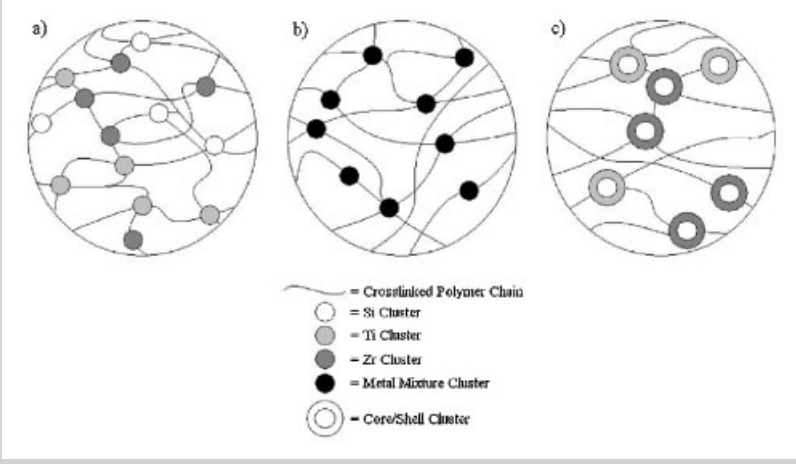

Possible network compositions of the cured material (a) specific metal-oxo-clusters, (b) hetero-bonded metal-oxo-clusters, and (c) core/shell type metal-oxo-cluster configuration.

Effect of Mixed Sol-Gel Precursors on the Metal-Oxo Phase Within a UV-Curable Silicone Hybrid Material

*David P. Dworak, Mark D. Soucek**

The University of Akron, Department of Polymer Engineering, Akron, OH 44325, USA
Fax: +1 330 258 2339; E-mail: msoucek@uakron.edu

Received: February 1, 2006; Revised: May 10, 2006; Accepted: May 12, 2006; DOI: 10.1002/macp.200600051

Keywords: hydrolysis/condensation; metal-oxo-clusters; nanophase reinforcement; NMR; PM-FTIR; polycondensation; sol-gel; solid state ^{13}C NMR; solid state ^{29}Si NMR

Introduction

The sol-gel method is one of the most widely used methods for the synthesis of inorganically modified organic and/or inorganic based materials.[1–3] These hybrid materials have the combined desirable properties of both the inorganic (hardness, durability, and thermal stability) and polymeric (flexibility and toughness) components within a single network. Traditionally, this ''combination of properties'' is accomplished via a step-growth polymerization, comprising hydrolysis and polycondensation reactions of organoalkoxysilanes which have been incorporated into the

polysiloxane prior to casting. Upon curing, the organoalkoxysilanes will react in situ with atmospheric moisture and form a three-dimensional network in the process.

Most of the hybrid materials are prepared by the sol-gel process using organoalkoxysilanes as precursors. In addition, many organosiloxane-based materials use siloxanes as the sole sol-gel component. The incorporation of a mixture of sol-gel precursors and other co-reactants into the hybrid material is anticipated to provide materials with a number of functions or capabilities.[4–7] This approach of in situ formation of nanosized metal-oxo-clusters can offer UV-stability, mechanical reinforcement, and provide corrosion protection.[8–12] Also, application of hybrid materials in the aerospace industry could provide protection against radiation as well as high energy particles that are present in a space environment.[13]

In addition to the metal alkoxides reacting with each other, the polymer can be modified with pendant alkoxy silane groups, which can act as a coupling agent nucleating the development of metal-oxo-cluster growth. Thus, the in situ formed systems are well dispersed in comparison with post-added nanoparticles. Furthermore, the alkoxy silane groups can self-condense to form crosslinks. Once cured the material should form an interlocking hybrid network consisting of a crosslinked polymer phase with interconnected silicon/metal-oxo-clusters.[14] The number of metal oxide linkages (M–O–M) in the final composition of the material is dependent upon the degree to which the hydrolysis and polycondensation reactions proceed. The extent of completion of the overall sol-gel process is an important factor in the determination of the final structure for all types of hybrid materials. Metal alkoxides are useful not only for the incorporation of the nanosized inorganic components but also for their catalytic effect on the hydrolysis and condensation reactions. This catalytic effect of metal alkoxides can prevent the formation of volatile low molecular weight species such as short-chain oligomers and cyclic siloxanes during the condensation reactions.[15,16] Figure 1 is a depiction of the interconnecting network formed between the cured polysiloxane and the metal-oxo-clusters.

Raman spectroscopy, small-angle X-ray scattering, ^{17}O solid state MAS NMR, and various mechanical tests have been employed to study the physical/mechanical properties in addition to the morphology of modified sol-gel materials.[17–21] These studies were performed as a function of reaction conditions and composition and found the materials to be transparent and homogenous with the modifying component. The ^{17}O solid state NMR studies found the parameters (C_Q, T_1, etc.) for Si–O–Si and Si–OH fragments within a sol-gel material, however no information was presented on the overall network structure.[13] In addition, the physical and mechanical properties of these modified materials were found to be appreciably different from the unmodified components.[9–11]

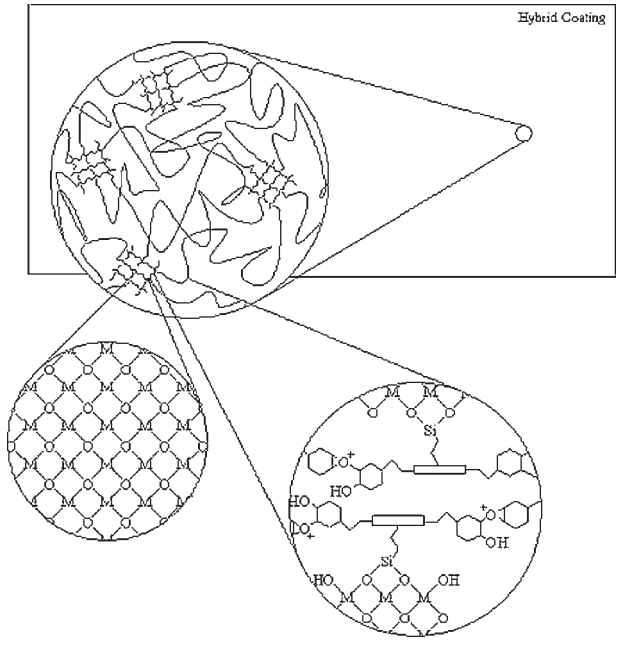

Figure 1. Depiction of nanophase reinforcement in hybrid materials.

In this study, a mixed metal-oxo hybrid material will be investigated with a cycloaliphatic epoxide and triethoxysilane functionalized polysiloxane of high molecular weight as the continuous phase. Polysiloxanes with three alkyl substitutions (methyl, cyclopentyl, and cyclohexyl) were prepared.[22] The homopolymerization of the cyclohexyl epoxide and hydrolysis of the sol-gel precursors will be cured at ambient temperature via a cationic photoinitiator. Mixtures of various sol-gel precursors, tetraethylorthosilicate (TEOS) oligomers, titanium(IV) *iso*-propoxide (TiP), zirconium(IV) propoxide (ZrP), and zinc acetate (ZnAc) were added to the polysiloxane. It is crucial to investigate the inter-reactivity of nanoparticle precursors and morphology colloids, derived from mixed precursors by in situ preparation of nanocomposite materials, for the control of end properties and ultimately the fabrication of smarter multifunctional materials.

Experimental Part

Materials

Substituted polysiloxanes were synthesized and functionalized prior to this experiment (Figure 2).[22] Zirconium(IV) propoxide, 70 wt.-% solution in 1-propanol, titanium(IV) *iso*-propoxide (97%), TEOS (98%), zinc acetate (99.99%), and toluene (99.5%) were purchased from Aldrich Chemical Company and used as supplied. Tetraethoxysilane oligomers were synthesized and characterized prior to use.[2] Toluene was distilled in order to eliminate any impurity and stored with molecular sieves (4A, beads, 8–12 mesh). Irgacure 250 was supplied by Ciba Specialty Chemicals and used as received. Aluminum mill finish 2024-T3 (3×6 in^2) panels

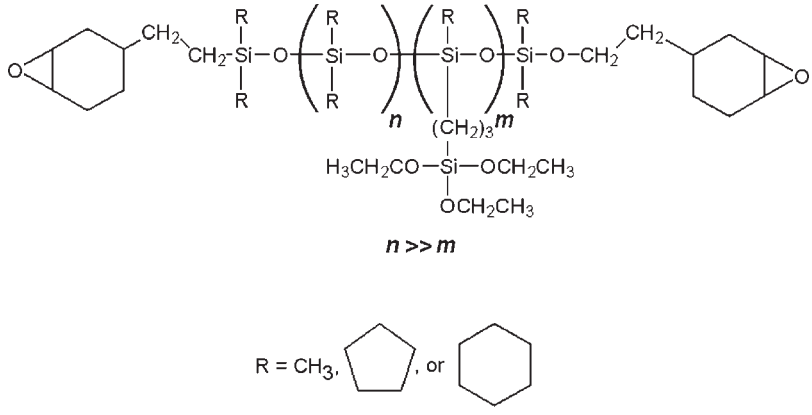

Figure 2. Structure of substituted polysiloxanes utilized in coating formulation.

were obtained from a Q-panel. All materials were transferred and weighed in a dry box under argon.

Film Preparation and Application

In a dry box, the substituted polysiloxane (≈3.0 g) was added to a glass vial, which was pre-heated at 100 °C for 15 min prior to use. Dry toluene (20 wt.-%) was then added and thoroughly mixed. Zirconium(IV) propoxide (5 wt.-%), titanium(IV) *iso*-propoxide (5 wt.-%), and TEOS oligomers (5 wt.-%) were added and mixed. The zinc acetate was dissolved in boiling absolute ethanol (5 wt.-%) prior to use and added to the mixture. Irgacure 250 (3 wt.-%) was added and the entire solution was well mixed. The solutions containing cycloaliphatic substituted polysiloxanes required 6 wt.-% of Irgacure 250.

A low humidity environment (RH ≈ 15%) was created via the aid of a nitrogen filled tent encapsulating the UV-curing chamber. The solution was applied to acetone rinsed aluminum Q-panels (3×6 in^2) with the aid of a draw down bar (2 mil). A Fusion UV-curing chamber (F300SQ Series) with a belt speed

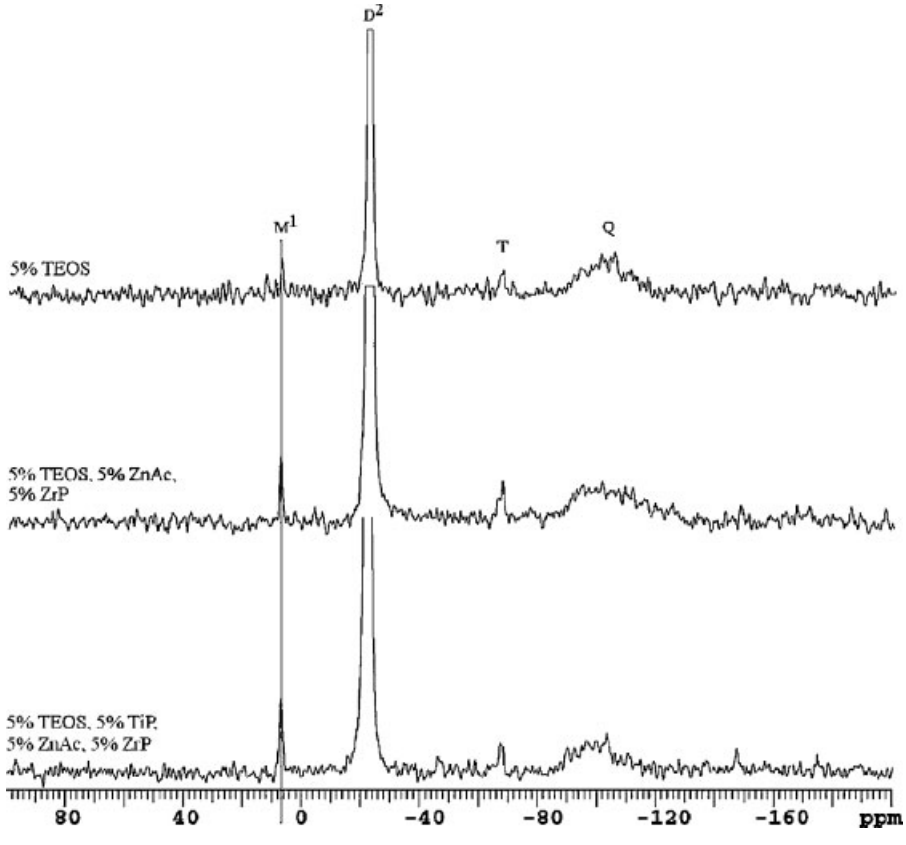

Figure 3. Solid state ^{29}Si spectra of UV-curable polydimethylsiloxane functionalized with triethoxysilane and incorporated with various sol-gel precursors.

of 55 ft · min^{-1} was used to cure the polysiloxanes with a UV-source (mercury arc bulb, ≈150 mW · cm^{-2}). The polysiloxanes incorporated with metal alkoxides required additional cure time and were cured with a belt speed of 10 ft · min^{-1}. All samples were tested 24 h after curing to allow for dark cure and the sol-gel process to complete.

X-ray Photoelectron Spectroscopy (XPS)

The XPS was completed on a Kratos Model ES3000 with a non-monochromatic 120 Watt Al K-Alpha radiation source under a 10^{-8} torr vacuum. Samples were cast and cured onto masking tape for ease of sampling and had an average thickness of 15.6 ± 2.7 μm.

Solid-State ^{13}C and ^{29}Si NMR Analysis

Solid-state spectra were obtained on a Varian INOVA 200 using zirconia rotors with Kel-F end caps operating at 200 MHz (4.7 T). All samples were subjected to magic angle spinning rates of 5 kHz and had a crosspolarization time of 53 kHz and a relaxation delay of 2.0 s. Contact time of ^{29}Si spectra was 3 ms and PW90 = 5.8 μs. The average time to obtain a ^{29}Si spectra was 4 h and 42 min. ^{13}C spectra contact time was 1 ms and PW90 = 4.7 μs. The average time to obtain a ^{13}C spectra was 2 h and 20 min. Hexamethylbenzene (HMB) methyl peak was used as an internal standard and referenced to $\delta \approx 17.3$ ppm for ^{13}C spectra and ^{29}Si used 3-(trimethylsilyl)-1-propanesulfonic acid sodium salt (DSS) referenced to $\delta = 1.46$ ppm relative to TMS at $\delta = 0$ ppm.

Phase-Modulated FT-IR (PM-FTIR) Analysis

Absorbance spectra of UV-cured spin cast films on aluminum Q-panels were obtained using a NEXUS 870 Nicolet Research FT-IR. The incoming FT-IR beam was passed through a wire grid polarizer creating a p-polarized beam, which was then sent through a ZnSe photoelastic modulator (PEM), and finally focused onto the sample at an incident angle of 75°. After the sample, the beam was collected onto a single ZnSe lens and focused onto a detector (Nicolet type MCTA) that was cooled with liquid nitrogen prior to use. All spectra were subjected to 2 000 scans with a resolution of 4 cm^{-1}. The entire optical layout fitted under a nitrogen purged cover.

Results

The intention of this study was to investigate the final composition of the pre-ceramic phase formed via the sol-gel process within a UV-curable polysiloxane material that contains various sol-gel precursors. A cationic photoinitiated route was chosen to polymerize both the silicon phase and catalyze the sol-gel reactions where the presence of water is necessary to initiate the sol-gel process. To investi-

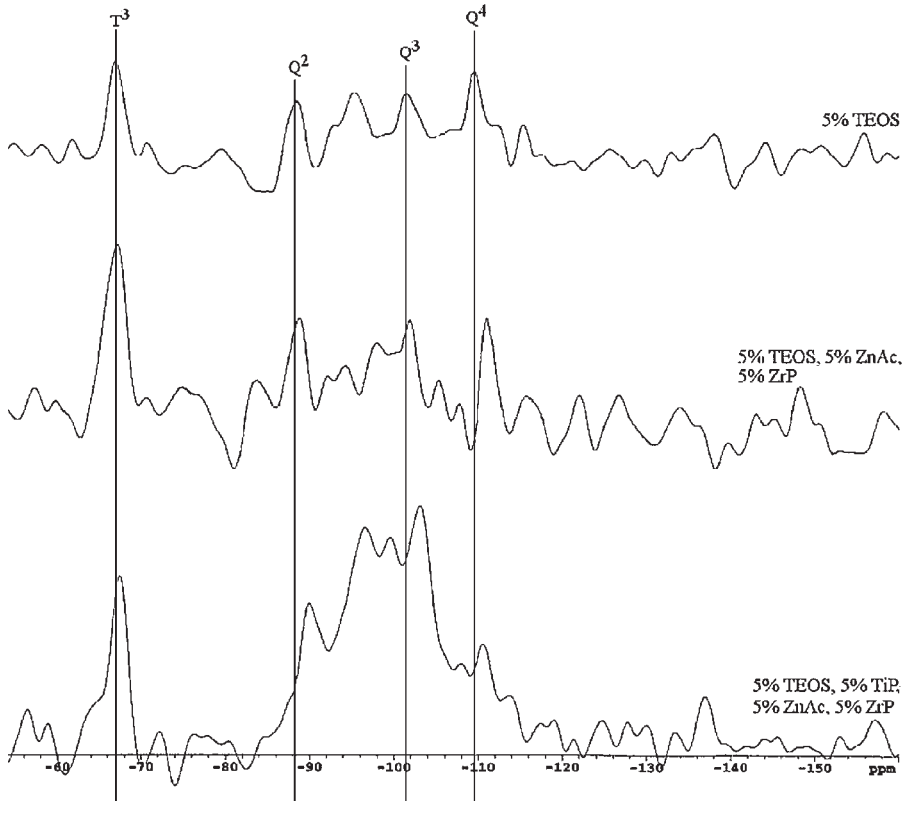

Figure 4. Expanded solid state ^{29}Si spectra of UV-curable polydimethylsiloxane functionalized with triethoxysilane and incorporated with various sol-gel precursors.

gate the structure of the network formed within the hybrid materials solid state ^{29}Si NMR and solid state ^{13}C NMR were used in conjunction with PM-FTIR spectroscopy and XPS. The sensitivity of the ^{29}Si nuclei to their electronic, atomic, and molecular environments provides an accurate chemical shift dispersion range for the analysis of organosilicon compounds.[20] Solid state ^{29}Si spectra have shown that isotropic chemical shifts are dependent upon the degree of condensation of the silicate structures and that these shifts compare appreciably to the solution spectra of the same structures.[23–25] Phase-modulated FT-IR allows, specifically, for the internal structure of the crosslinked network to be analyzed as opposed to the surface, providing more insight in to the development of the hybrid material.[26,27] Elemental identification was performed by way of XPS to compare theoretical and actual atomic composition percentage. XPS was also performed in order to verify the presence of the incorporated sol-gel precursors.

Solid-State ^{29}Si NMR

Figure 3 is the solid-state ^{29}Si NMR spectra for the methyl substituted triethoxysilane functionalized polysiloxane with various sol-gel precursor mixtures. To study the effects that zirconium and titanium sol-gel precursors have on the internal structure, the spectra are being compared to a sample incorporated only with TEOS. The M^1 units can be observed at $\delta \approx 8.0$ ppm on each of the three samples, which represents the terminal silicon atoms of the polysiloxane chain attached to the cycloaliphatic epoxy.[28] It is important to note that the M^1 peak does not shift from sample to sample. The prominent peak at $\delta \approx -22$ ppm represents the repeating D^2 units of the polysiloxane chain.

In analyzing the solid-state ^{29}Si NMR results, Figure 3 displays an absence of shifting in the "M" and "D" peaks.[28] This consistency in range was not observed for the "T" and "Q" silicon atoms and indicates that the silicon-oxo bridges that were formed during the sol-gel process have bonded with another metal other than silicon and have formed a hetero-bonded interlocking network.

Figure 4 is an expansion of the NMR spectra in Figure 3 to elucidate the T and Q groups. Figure 4 clearly shows that the triethoxysilane groups have fully reacted as a result of the T^3 peaks present at $\delta \approx -67$ ppm in all three spectra. If the triethoxysilane group reacted only partially, then T^1 or T^2 peaks would be observed below $\delta \approx -67$ ppm. Figure 3 also shows Q^2, Q^3, and Q^4 peaks for all three samples. The Q^1 peak appears near $\delta \approx -80$ ppm and is not observed in any of the three samples.[26] An important observation in Figure 4 is that the samples that contain ZrP, TiP, and ZnAc

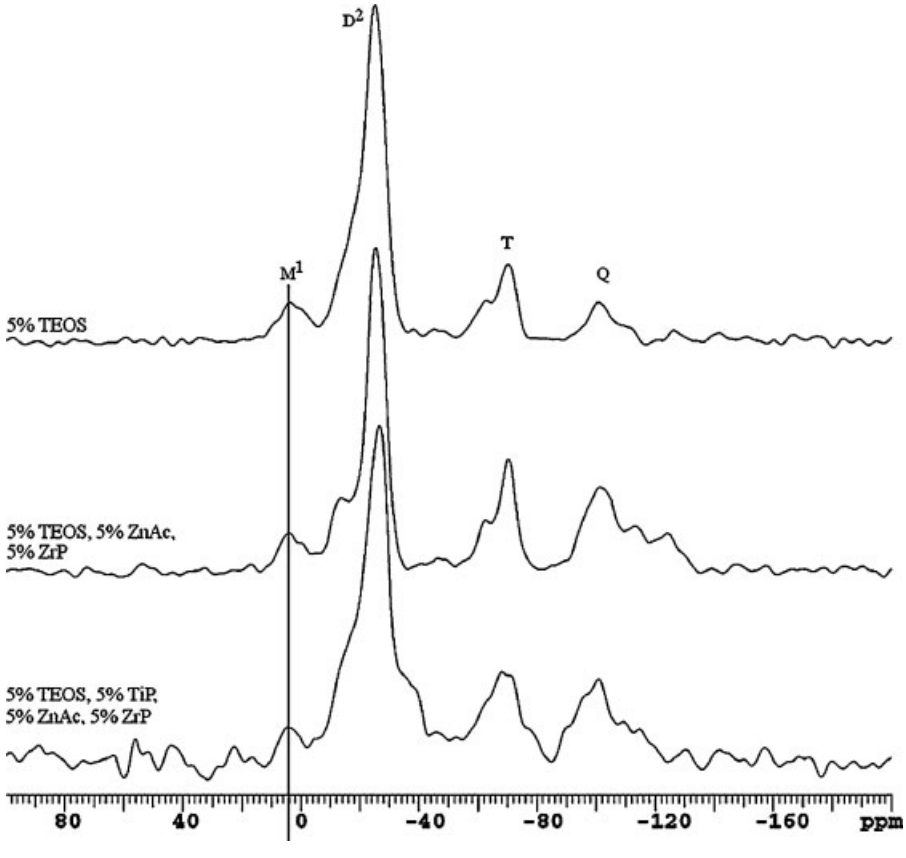

Figure 5. Solid state ^{29}Si spectra of UV-curable polydicyclopentylsiloxane functionalized with triethoxysilane and incorporated with various sol-gel precursors.

show a slight shift, from $\delta \approx 0.5$ to $\delta \approx 1.1$ ppm, of the Q peaks. The Q^4 peaks, for example, in the samples that contain ZrP, TiP, and ZnAc would be consistent with the TEOS Q^4 peak if the substitutions about the oxygen atoms were all silicon; however, this is not observed. This chemical shift cannot be caused by the influence of the neighboring Ti atom on the chemical shift of the Si atom. This influence contributes to a shift of $\delta \approx 0.3$ ppm at the most.[28] The high field shift is expected on account of the heteroatom Si–O–M bonds. High field shifts have been observed for the Si atoms in Ti–O–Si–O–Ti bonds of various cyclic titanodiphenylsiloxanes.[29] This shift is observed for the Q units, but is not observed in the M and D units, which further supports the concept of heteroatom bonded metal-oxo-clusters. The T^3 peak in Figure 3 does not display the magnitude in shifts that are observed with the Q peaks, which could indicate that alkoxy silane Si predominantly reacts with TEOS and not with the other metal sol-gel precursors. Since the T and Q units are of great interest, Figure 4 represents an expanded spectrum of those two regions.

Figure 5 shows the full solid state ^{29}Si spectra for the cyclopentyl substituted triethoxysilane functionalized polysiloxane with a variety of sol-gel precursors while Figure 6 is an expanded spectrum of the T and Q regions. As shown in Figure 5, the M^1 and D^2 units of the polysiloxane chain are within the expected range. Not surprisingly, there is a slight upfield shift as a result of the large and bulky cyclopentyl groups attached to the Si atoms. Figure 6 shows the expanded spectral region of the T and Q peaks and when compared to the T region in Figure 4, an additional T^2 peak was observed.

Figure 6 shows an additional peak in the T region of the spectra. This additional T^2 peak indicates that the

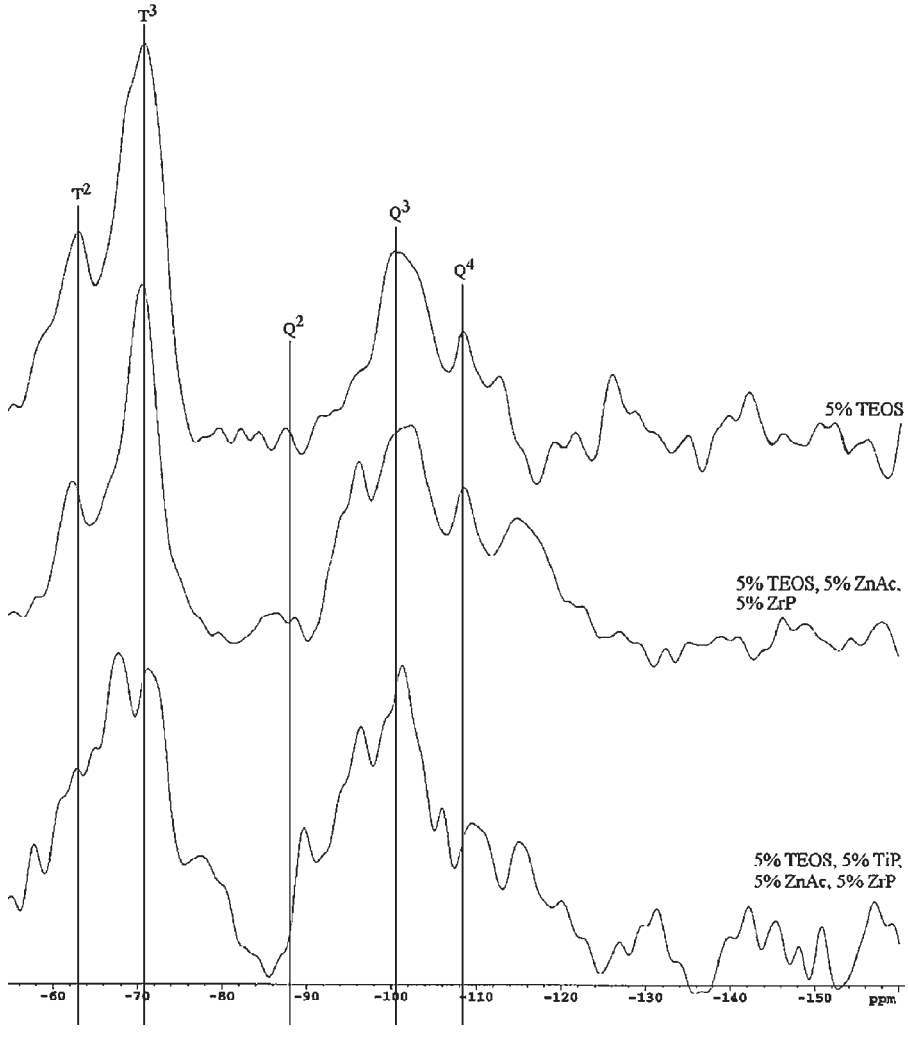

Figure 6. Expanded solid state ^{29}Si spectra of UV-curable polydicyclopentylsiloxane functionalized with triethoxysilane and incorporated with various sol-gel precursors.

triethoxysilane functionality did not undergo full substitution and still possesses at least one or more $-OCH_2CH_3$ groups. The Q unit region displays peaks for Q^2, Q^3, and Q^4 units. The TEOS containing sample does not show a prominent peak for Q^2 unlike the TiP, ZrP, and ZnAc samples. This would indicate that the sol-gel process progressed more towards completion by yielding more Q^3 and Q^4 units. This trend was not observed in the methyl substituted polysiloxane sample (Figure 3 and 4).

Solid State ^{13}C NMR

Figure 7 is a solid state ^{13}C NMR of UV-cured polydimethylsiloxane functionalized with triethoxysilane and a mixture of sol-gel precursors. The spectra show the peaks for the methyl (≈2 ppm) and cycloaliphatic epoxide carbons ($\delta \approx 32$ and $\delta \approx 77$ ppm), respectively. Closer examination of Figure 7 reveals two peaks at $\delta = 58.4$ and $\delta = 18.4$ ppm, which represent the ethoxy carbons of TEOS. The peak at $\delta \approx 18$ ppm represents the carbon **R**–Si–$(OR)_3$ of the T unit. The carbons of the propoxide and *iso*-propoxide groups appear in at $\delta \approx 45$ and $\delta \approx 28$ ppm based on ^{13}C predicted resonances.

Figure 8 shows the solid state ^{13}C NMR of UV-cured polydicyclopentylsiloxane functionalized with triethoxysilane and various sol-gel precursors. Similar to Figure 7, Figure 8 shows that carbon atoms of residual ethoxy groups are present and peaks that would reveal the presence of propoxide and/or *iso*-propoxide groups are not observed. Both Figure 7 and 8 show that as the number of sol-gel precursors increase the intensity of the ethoxy carbons peak decreases. This could be a result of the addition of more species to undergo hydrolysis and condensation reactions with the oligomerized TEOS. Solid state ^{13}C NMR was able to determine the specific alkoxy groups still present in the final crosslinked network by being able to identify specific carbon atoms.

Phase-Modulated FT-IR

In order to get a better understanding of the composition of the metal-oxo-clusters, PM-FTIR was utilized to confirm the presence of M–O–M and/or Si–O–M clusters. Formation of Si–O–Zr bonds has been identified through the band near 960–950 cm^{-1}, while the Si–O–Ti band is near 920 cm^{-1}.[29–31] These absorbances are slightly lower than

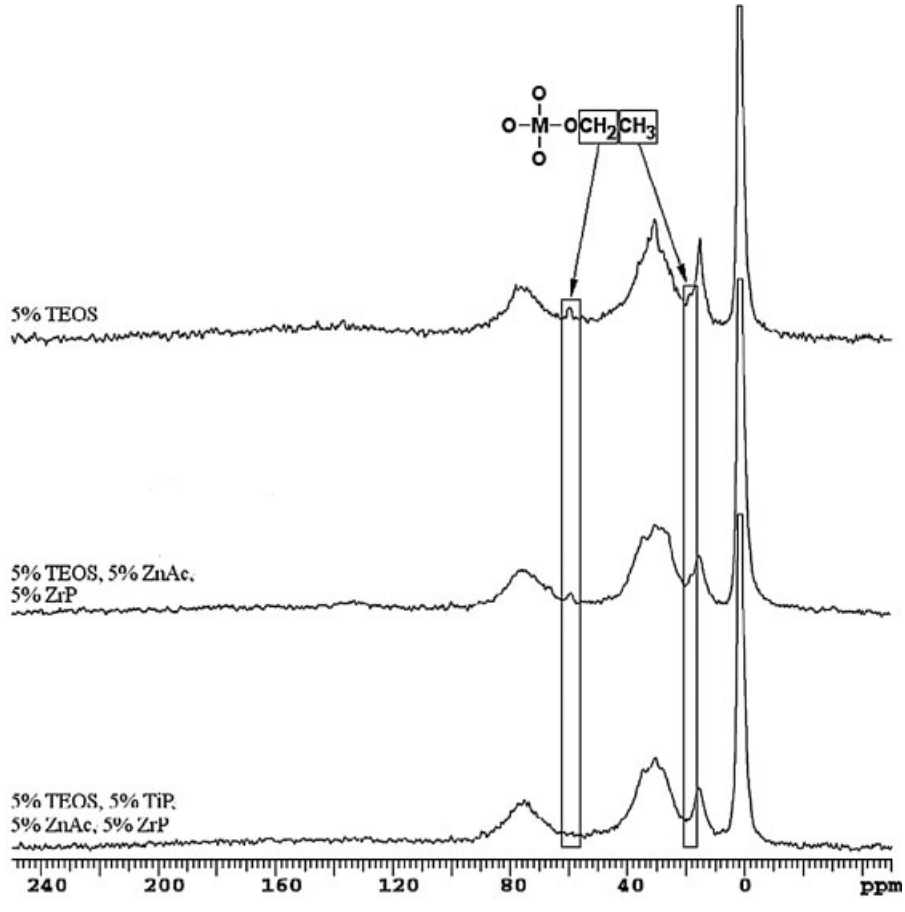

Figure 7. Solid state ^{13}C NMR spectra of UV-curable polydimethylsiloxane functionalized with triethoxysilane and incorporated with various sol-gel precursors.

the Si–O–Si frequency due to the presence of the metal which perturbs the vibration of the silicon atom and is a good indication of the formation of heteroatom bonds.

Siloxanes (Si–O–Si) give a characteristic doublet between 1 100 and 1 000 cm^{-1}; however, using that region as the focus of confirming the presence of silicate clusters is injudicious since the polymer backbone is comprised of repeating Si–O bonds. Therefore, the region of 1 100 to 400 cm^{-1} was examined in order to identify the composition of the oxo-clusters. This region contains the vibration range of Si–O–M and M–O–M species. Absorption peaks present near 500–480 cm^{-1} are characteristic of the vibrations of Zr–O–Zr bonds and peaks in the region of 620–600 cm^{-1} represent Ti–O–Ti vibrations.[31–33] Zinc oxide displays a faint absorbance near 700 cm^{-1}. The Si–O–Si bond vibration also gives a weak absorbance in the range of 650–500 cm^{-1}, but overlaps with the polysiloxane based polymer backbone.[26] Figure 9 presents the PM-FTIR spectra of UV-curable polydimethylsiloxane functionalized with triethoxysilane and a mixture of sol-gel precursors and shows strong indication of mixed metal-oxo-clusters due to the presence of the absorbances between 1 000 and 900 cm^{-1}.

Figure 10 and 11 are of the cycloaliphatic substituted polysiloxane, functionalized with triethoxysilane and treated with sol-gel precursors. Similar to Figure 9 the presence of hetero-bonded metal-oxo-clusters are observed through the prominent absorbances between 1 000 and 900 cm^{-1} in the samples that contained the sol-gel precursors. The zinc oxide peak is also observed in each of the PM-FTIR spectra. Organic groups such as cycloaliphatic and methyl groups are also present. Figure 9–11 show strong indication of mixed metal-oxo-clusters due to the presence of the absorbances between 1 000 and 900 cm^{-1}. The weak absorbance at 650 cm^{-1} reveals the presence of Si–O–Si linkages. The zinc oxide band is also observed.

XPS

Table 1 gives a comparison between the theoretical and actual atomic percentage for the sample, and Figure 12 shows the XPS spectra for the cured cyclohexyl-substituted polysiloxane with 5 wt.-% of each of the sol-gel precursors and displays trace amounts of titanium and zirconium metal along with the more prominent carbon, oxygen, and silicon.

A disagreement was observed between the actual and theoretical atomic composition values. Although the major binding energy peak of zinc is beyond 1 000 eV (1 021 eV), its presence could not be determined from the XPS spectra. The other zinc spectral lines (3d, 3p, and 3s) could also not

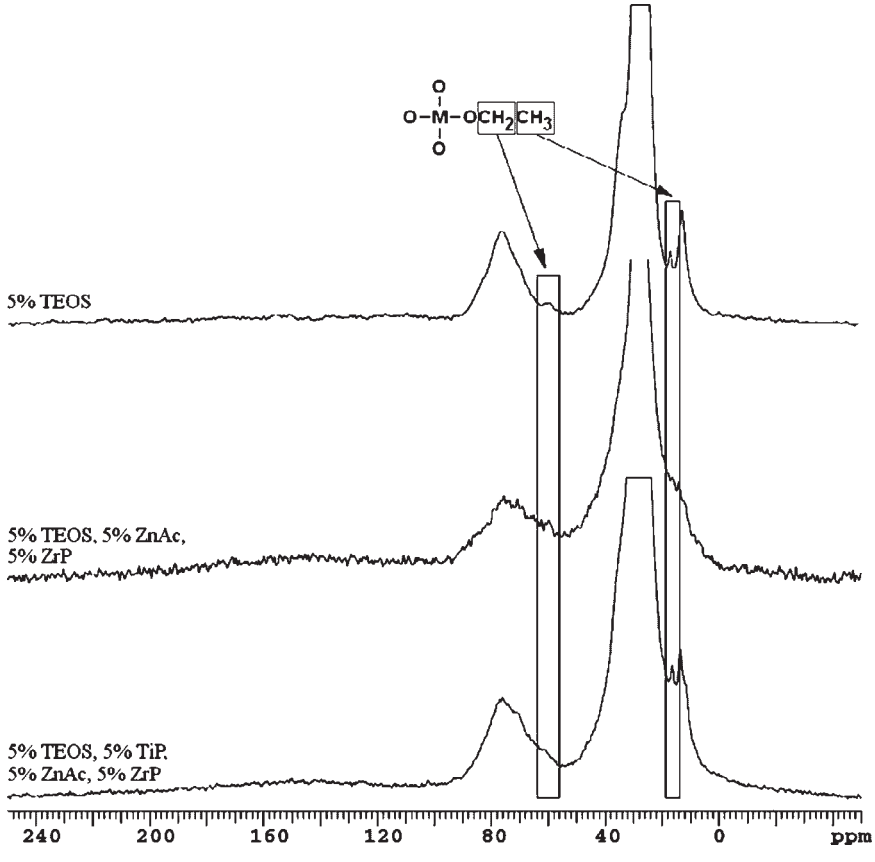

Figure 8. Solid state ^{13}C NMR spectra of UV-curable polydicyclopentylsiloxane functionalized with triethoxysilane and incorporated with various sol-gel precursors.

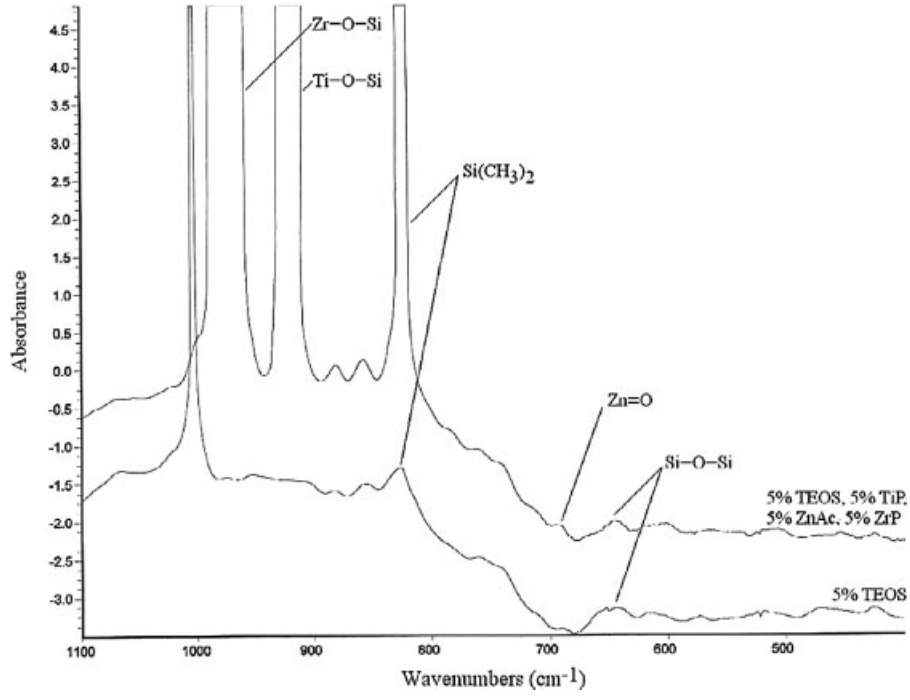

Figure 9. PM-FTIR spectra of UV-curable polydimethylsiloxane functionalized with triethoxysilane and incorporated with various sol-gel precursors.

be observed due to such a low concentration of the sol-gel precursor. The XPS atomic composition analysis yielded discrepancies between the actual and theoretical values. Incorporating the sol-gel precursors/metal-oxo-clusters would prove complex in that the degree of conversion of the sol-gel precursors would have to be assumed at 100%, but solid-state ^{13}C NMR results show that this does not occur. The actual silicon composition is slightly higher due

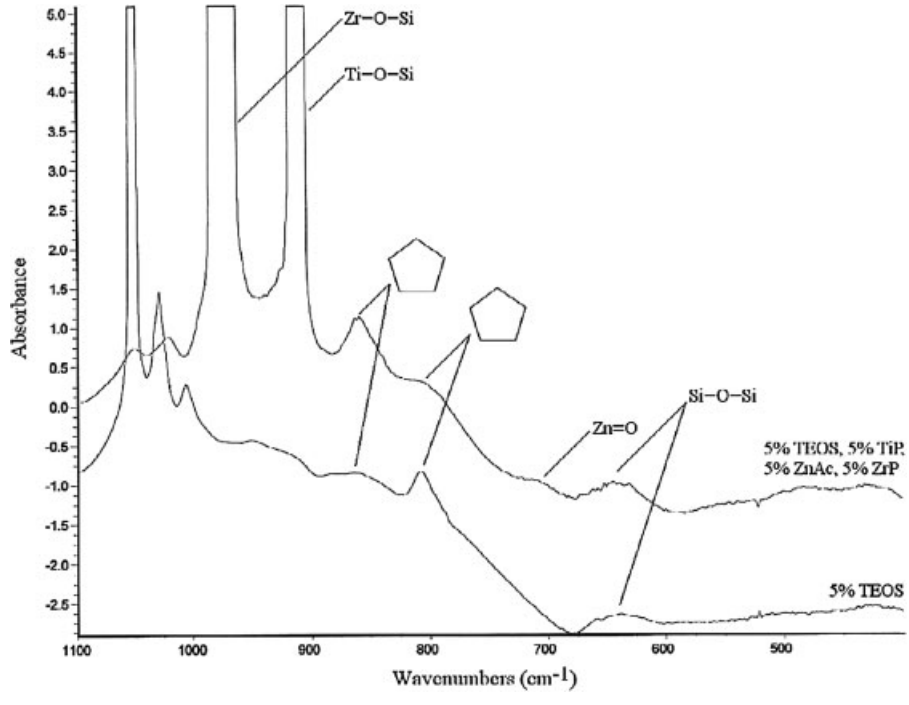

Figure 10. PM-FTIR spectra of UV-curable polydicyclopentylsiloxane functionalized with triethoxysilane and incorporated with various sol-gel precursors.

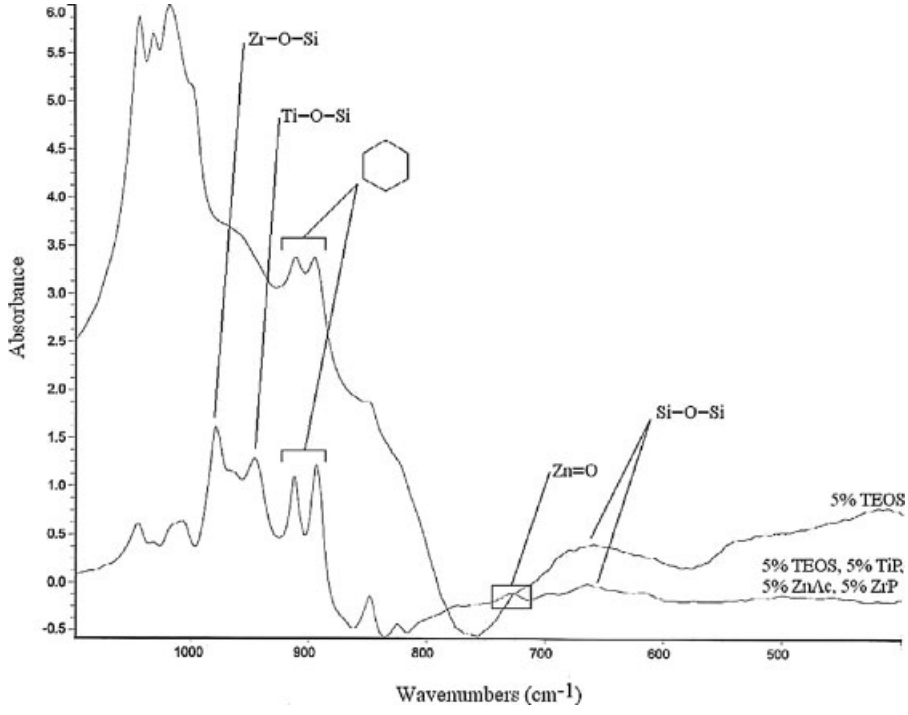

Figure 11. PM-FTIR spectra of UV-curable polydicyclohexylsiloxane functionalized with triethoxysilane and incorporated with various sol-gel precursors.

to the presence of the sol-gel precursor TEOS, and when compared to the low composition values for the titanium and zirconium an increase of 0.29 is not unexpected. The largest difference in the composition values is for titanium and zirconium. A concentration of 5wt.-% sol-gel precursor may not provide enough metal atoms to get a distinct spectral line. However, evidence of zirconium and titanium peaks reinforces the presence of the metal-oxo-clusters.

Discussion

Some previous studies have shown that mixed sol-gel precursors can form hetero-bonded oxo-clusters.[34–36] The hydrolysis and condensation rates for the sol-gel precursors are different; mixing prior to application disperses the metal alkoxides within the polymer phase and does not usually allow for single domain formation. As a result, the metal alkoxides can initiate the sol-gel process with the nearest precursor which should allow for hetero-bonded oxo-clusters.

By utilizing PM-FTIR and solid state ^{29}Si and ^{13}C NMR in tandem, the various types of silicates/metalates formed during the sol-gel process were distinguished. Either a homogenous or heterogeneous distribution of structural units at the molecular level may be beneficial depending on the intended usage.[37] Figure 13 depicts three different possible ways in which the metal-oxo-clusters could form. Figure 13(a) illustrates that each individual sol-gel precursor reacts with itself to form independent oxo-clusters composed of a specific metal oxide (Zn–O–Zn). Figure 13(b) depicts precursors reacting with each other to form clusters of hetero-bonded metal oxides (Zn–O–Si, Zr–O–Si, etc.). Finally, Figure 13(c) portrays a ''core/shell'' type structure with one sol-gel precursor reacting with itself followed by the addition of another precursor.

The solid state ^{29}Si NMR displays a range of T and Q peaks that have shifted as a result of incorporating a mixture of sol-gel precursors. Mixing the sol-gel precursors prior to casting the films allows for complete dispersion amongst the polysiloxane matrix. This allows for the sol-gel precursors to avoid single domain formation and form the hetero-bonded metal-oxo-clusters observed in the solid state ^{29}Si NMR spectra. The role of the medium plays an important role in the degree of completion of the hydrolysis and condensation reactions. Higher molecular weight species, such as the methyl substituted polysiloxane sample

Table 1. XPS analysis of cyclohexyl substituted polysiloxane with sol-gel precursors.

Element identification	Atomic composition	
	Actual	Theoretical
	%	%
C (1*s*)	75.91	78.50
O (1*s*)	16.25	11.40
Si (2*p*)	7.39	7.10
Ti (2*p*)	0.29	1.50
Zr (3*d*)	0.16	1.50

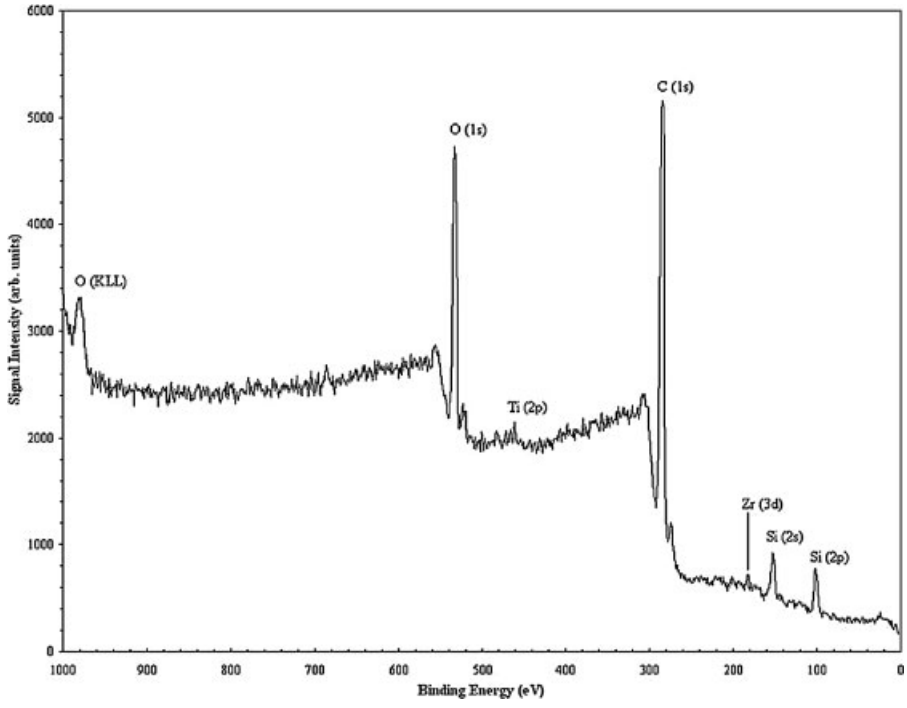

Figure 12. XPS spectra of cyclohexyl substituted polysiloxane cured with Ti, Zr, and Zn sol-gel precursors.

($\approx$45 000 g $\cdot$ mol^{-1}), possesses longer polysiloxane chains and have a higher viscosity. The cyclopentyl and cyclohexyl substituted polysiloxane samples have a molecular weight of $\approx$36 000 g $\cdot$ mol^{-1}. The presence of longer polysiloxane chains and a higher viscosity media may have prevented the completion of the sol-gel process. In addition to viscosity, the larger cycloaliphatic backbone substituents could change the hydrophobicity of the medium and prevent complete hydrolysis of the incorporated sol-gel precursors.

These factors could have contributed to the higher concentration of residual ethoxy groups found in the cycloaliphatic substituted polysiloxane. The cycloaliphatic

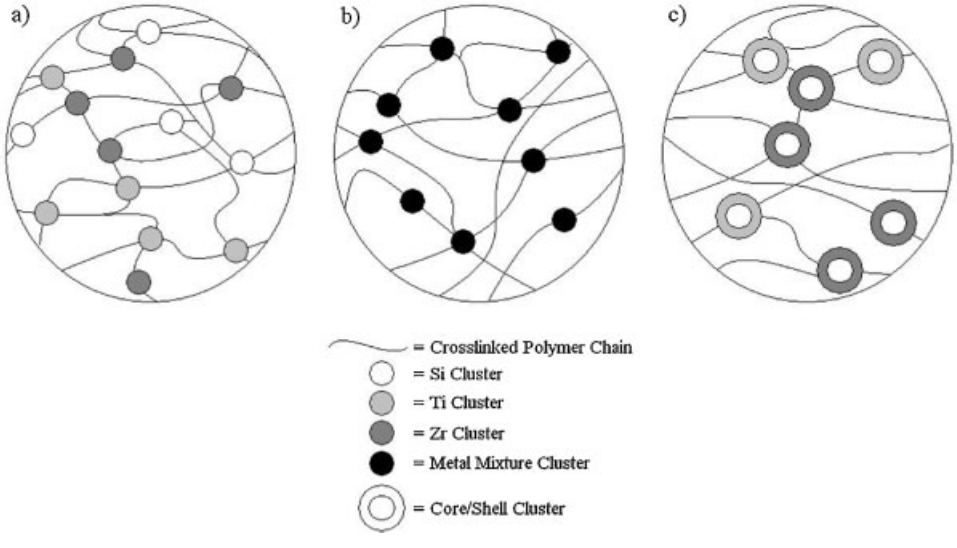

Figure 13. Possible network compositions of the cured material (a) specific metal-oxo-clusters, (b) hetero-bonded metal-oxo-clusters, and (c) core/shell type metal-oxo-cluster configuration.

groups are more hydrophobic than a methyl group and may have prohibited the amount of water necessary for the complete hydrolysis of the alkoxide species. The cyclopentyl groups could provide a more hydrophobic character to the media and prevent the complete hydrolysis and condensation of the triethoxysilane functionality since the T^3 is still the principle peak for that region and that the methyl substituted polysiloxane did not reveal an additional T^2 peak.

Evidence of hetero-bonded metal-oxo-clusters is further reinforced through the utilization of PM-FTIR and XPS. The range of the M–O–M species (620–480 cm^{-1}) does not reveal the presence of homo-bonded metal-oxo-clusters, which indicates that Figure 13(a) and (b) are not the predominant structures. Therefore, evidence from PM-FTIR spectra would indicate that the final composition of the metal-oxo-clusters are hetero-bonded (Scheme 2). Phase-modulated FT-IR was able to identify the structure of the metal-oxo-clusters by detecting the specific absorbance bands for hetero-bonded metal-oxo-clusters. From Figure 9–11 the spectra show that the synthetic route used leads to the formation of hetero-bonded silicon-oxo-clusters. The results from XPS identified the predicted elements, but the low concentration of sol-gel precursors made the chemical composition of the final structure difficult to resolve. This was not surprising since the polymeric binder dominates the film-substrate interface.[38]

The ability to control the composition of the metal-oxo-clusters developed from hydrolysis and condensation reactions is important for in situ formation of nanocomposite smart materials. The affinity towards a specific metal alkoxide reacting with itself does not appear to be a factor during the sol-gel process within this specific system. Mixed titania-silica oxides prepared by the sol-gel process in chitosan have also displayed this trend.[26] Finally, hydrolyzed glycidoxypropyltrialkoxysilane and titanium-alkoxide form hetero-bonded Si–O–Ti structures via the sol-gel process, although increasing amounts of water homo-bonded (Ti–O–Ti) prevailed.[32] The control of the metal-oxo-colloid formation within a polymer matrix will be the subject of further investigation with the purpose of forming 13a and 13c structures with an in situ approach.

Conclusion

Solid state ^{13}C and ^{29}Si NMR with PM-FTIR and XPS were used to explicate the composition of metal-oxo-clusters formed from the sol-gel process within a UV-curable polysiloxane. The pendant triethoxysilane hydrolysis and condensation reactions of the sol-gel precursors were a function of the alkyl groups substituents attached to the polysiloxane backbone. It was proposed that the viscosity and hydrophobicity of the polysiloxane were the primary factors in determining the extent of the in situ sol-gel process. The presence of hetero-bonded silicate structures (Si–O–M) was indicated by ^{29}Si NMR and corroborated by PM-FTIR. Therefore, the results from the solid state NMR and PM-FTIR indicate that the metal alkoxides do not seem to have a preference regarding the metal alkoxide with which they can react as a result of the formation of Si–O–M linkages during the sol-gel process.

Acknowledgements: The authors would like to gratefully thank Dr. *Todd Wagner* of the University of Akron's Chemistry department for his solid state NMR contribution. Thanks to Dr. *Jun Hu*, also of the University of Akron's Chemistry department, for use of his PM-FTIR spectrometer. The authors also appreciate Dr. *Rex Ramsier* and *Nenad Stojilovic* of the University of Akron's Physics department for the XPS contribution.

[1] C. J. Brinker, G. W. Scherer, "*Sol-Gel Science*", Academic Press, San Diego 1990.
[2] M. D. Soucek, H. Ni, *J. Coat. Technol.* **2002**, *74*, 125.
[3] G. Teng, M. D. Soucek, *Macromol. Mater. Eng.* **2003**, *288*, 844.
[4] D. Deffar, G. Teng, M. D. Soucek, *Macromol. Mater. Eng.* **2001**, *286*, 204.
[5] G. Teng, M. D. Soucek, *J. Am. Oil Chem. Soc.* **2000**, *77*, 381.
[6] R. H. Glaser, G. L. Wilkes, *Polym. Bull* **1988**, *19*, 51.
[7] S. Dire, F. Babonneau, C. Sanhez, J. Livage, *J. Mater. Chem.* **1992**, *2*, 239.
[8] S. Hofacker, M. Mechtel, M. Mager, H. Kraus, *Prog. Org. Coat* **2002**, *45*, 159.
[9] D. Deffar, M. D. Soucek, *J. Coat. Technol.* **2001**, *73*, 95.
[10] H. Ni, A. H. Johnson, M. D. Soucek, J. T. Grant, A. J. Vreugdenhil, *Macromol. Mater Eng.* **2002**, *287*, 470.
[11] J. E. Mark, R. Abu-Hussein, G. S. Rajan, Y. T. Vu, M. K. Hassan, T. Kwee, K. A. Mauritz, C. Myers, *Polym. Prepr. Am. Chem. Soc., Div. Polym. Chem.* **2004**, *45*, 870.
[12] J. E. Mark, G. S. Rajan, G. S. Sur, D. W. Schaefer, G. Beaucage, *J. Polym. Sci., Part B: Polym. Phys.* **2003**, *41*, 1897.
[13] D. P. Dworak, M. D. Soucek, *Prog. Org. Coat.* **2003**, *47*, 448.
[14] R. H. Glaser, G. L. Wilkes, *J. Non-Cryst. Solids.* **1989**, *113*, 73.
[15] S. Dire, F. Babonneau, G. Carturan, J. Livage, *J. Non-Cryst. Solids* **1992**, *147–148*, 62.
[16] S. Dire, F. Babonneau, G. Carturan, J. Livage, *J. Mater. Chem.* **1992**, *2*, 239.
[17] H. Haung, B. Orler, G. L. Wilkes, *Polym. Bull.* **1985**, *14*, 557.
[18] D. Deffar, G. Teng, M. D. Soucek, *Macromol. Mater Eng.* **2001**, *286*, 204.
[19] R. H. Glaser, G. L. Wilkes, *Polym. Bull.* **1988**, *19*, 51.
[20] H. Haung, B. Orler, G. L. Wilkes, *Macromolecules* **1987**, *20*, 1322.

[21] E. R. H. van Eck, M. E. Smith, S. C. Kohn, *Solid State Nucl. Magn. Res.* **1999**, *15*, 181.
[22] D. P. Dworak, M. D. Soucek, *Macromolecules* **2004**, *37*(25), 9402.
[23] M. Mägi, E. Lippmaa, A. Samoson, G. Engelhardt, A. R. Grimmer, *J. Phys. Chem.* **1984**, *88*, 1518.
[24] G. Engelhardt, H. Jancke, E. Lippmaa, A. Samoson, *J. Organomet. Chem.* **1981**, *88*, 295.
[25] E. Lippmaa, M. Mägi, A. Samoson, G. Engelhardt, A. R. Grimmer, *J. Am. Chem. Soc.* **1984**, *102*, 4889.
[26] B. Barner, M. Green, E. Sáez, R. Corn, *Anal. Chem.* **1991**, *63*, 55.
[27] G. Steiner, H. Möller, O. Savchuk, D. Ferse, H. J. Adler, R. Salzer, *J. Mol. Struct.* **2001**, *563–564*, 273.
[28] D. Hoebbel, M. Nacken, H. Schmidt, *J. Sol-Gel Sci. Technol.* **1998**, *13*, 37.
[29] D. Hoebbel, M. Nacken, H. Schmidt, V. Huch, M. Veith, *J. Mater. Chem.* **1998**, *8*(1), 171.
[30] F. del Monte, W. Larsen, J. Mackenzie, *J. Am. Ceram. Soc.* **2000**, *83*(6), 1506.
[31] N. Agudjil, N. Benmouhoub, A. Larbot, ''*Elaboration and Characterization of Inorganic Membrane*'', Italian Association of Chemical Engineering, Milan (Unpublished).
[32] F. Sayilkan, H. Sayilkan, S. Erdemolu, S. Sener, M. Akarsu, *Turk. J. Chem.* **2004**, *28*, 27.
[33] H. Thoms, M. Epple, M. Fröba, J. Wong, A. Reller, *J. Mater. Chem.* **1998**, *6*, 1447.
[34] E. Pabón, J. Retuert, R. Quijada, A. Zarate, *Microporous Mesoporous Mater.* **2004**, *67*, 195.
[35] J. Miller, S. Johnston, E. Ko, *J. Catal.* **1994**, *150*, 311.
[36] R. Davis, Z. Liu, *Chem. Mater.* **1997**, *9*, 2311.
[37] H. Schmidt, ''*Chemical Processing of Advanced Materials*'', L. L. Hench, J. K. West, Eds., Wiley, New York 1992.
[38] Z. Zong, M. D. Soucek, C. Xue, *Poly. Sci. Part A* **2005**, *43*, 1607.

